Preparation and Characterization of Silver-Chitosan Nanocomposite Particles with Antimicrobial Activity

Jing An,[1,2] Qingzhi Luo,[1] Xiaoyan Yuan,[2] Desong Wang,[1] Xueyan Li[1]

[1]*School of Sciences, Hebei University of Science and Technology, Hebei, Shijiazhuang 050018, China*
[2]*School of Materials Science and Engineering, Tianjin Key Laboratory of Composite and Functional Materials, Tianjin University, Tianjin 300072, China*

Received 10 October 2008; accepted 6 April 2010
DOI 10.1002/app.33532
Published online 11 February 2011 in Wiley Online Library (wileyonlinelibrary.com).

ABSTRACT: A nanocomposite of silver nanoparticles (AgNPs) embedded in chitosan (Cts) matrix was successfully synthesized by crosslinking technology. Colloidal AgNPs formed *in situ* by chemical reduction of silver ions in presence of Cts showed a good stability. Transmission electron micrographs, X-ray diffraction patterns, and UV-visible spectra of Ag-Cts composite particles confirmed the formation of silver nanocrystals. Fourier transform infrared spectroscopy verified the presence of Cts as a stabilizing agent surrounded AgNPs. Thermogravimetric-differential scanning calorimeter analysis revealed Ag-Cts nanocomposite had a higher thermal stability than Cts. X-ray photoelectron spectroscopy suggested that the Ag-O bond in the nanocomposite coule lead to the tight combination between silver and Cts. Microbial experiments showed the nanocomposite had excellent and wide spectrum antibacterial properties, and were more efficient than either AgNPs or Cts alone for inactivating bacteria. Therefore, the resultant nanocomposite could be used as antimicrobial materials for medical and biological applications. © 2011 Wiley Periodicals, Inc. J Appl Polym Sci 120: 3180–3189, 2011

Key words: silver nanoparticles; chitosan; colloids; nanocomposite; antimicrobial activity

INTRODUCTION

Silver nanoparticles (AgNPs) have long been known to have powerful antimicrobial activities to nearly 650 trends of bacteria.[1,2] Because of the wide spectrum of antimicrobial property and the high activity with a low concentration,[3] they are widely applied in many biological and medical fields such as biosensors, wound healing materials, dental resin composites, cancer therapeutics,[4–7] and so on. Unlike pharmaceutical antibiotics, which provoke much bacterial resistance and destroy beneficial enzyme, AgNPs can leave these beneficial enzymes intact. The antimicrobial mode of AgNPs is that they attach to the bacterial cell wall and penetrate into cell membranes with compromised permeability, after that they bond DNA via thiol-containing proteins. Therefore, silver is absolutely safe for humans, plants, and all multi-celled living matters.[8,9]

Since more bacteria trends have demonstrated an increasing resistance toward antibiotics, AgNPs, as an antimicrobial agent, cannot do best singly and should be synthesized in the presence of other solid supports, such as polymers which can provide powerfully antimicrobial activity at the same environments.[10,11] Cts, being one of such nontoxic polymer, has attracted considerable interest due to its antimicrobial and antifungal activities.[12,13] Cts is one of the most abundant natural biopolymer derived by the deacetylation of chitin and the properties of biocompatibility, biodegradability, and bioactivity make Cts very attractive for a wide range of biomaterial, pharmaceutical, and medical applications.[14–16] According to hard and soft acid theory, polysaccharide is very efficient at chelating noble metals and widely used for extracting noble metals.[17,18] It has been reported that Cts can be used as stabilizing agent for silver and gold nanoparticles in the chemical reduction preparation method.[19–21] Twu et al. reported an approach to the preparation of Ag/Cts composite by using basic Cts suspension as stabilizing agent and reductant in the absence of other chemicals. They indicated that the size and distribution of the resultant composite were strongly dependent on the concentration of Cts and sodium hydroxide.[22]

In the work, the AgPNs in Cts colloid were synthesized by chemical reduction with $AgNO_3$ as

Correspondence to: D. Wang (dswang06@126.com).
Contract grant sponsor: Nature Science Foundation of Hebei Province, China; contract grant number: E2008000699.
Contract grant sponsor: Foundation of Hebei University of Science and Technology; contract grant number: XL200819.

precursor, Cts as stabilizing agent and sodium borohydride as reducing agent, respectively. Ag-Cts composite were successfully prepared by crosslinking technology. The Ag colloidal nanoparticles and Ag-Cts composite were characterized with UV-vis diffuse reflectance spectroscopy (UV-vis), transmission electron microscopy (TEM), scanning electron microscopy (SEM), Fourier transform infrared spectroscopy (FTIR), X-ray diffraction analysis (XRD), thermogravimetric-differential scanning calorimeter analysis (TGA-DSC), and X-ray photoelectron spectroscopy (XPS). In addition, antibacterial activities of the composite against different species bacteria were examined by the viable cell counting method.

EXPERIMENTAL

Materials

Cts (deacetylation degree 92%, $\overline{M}_w = 130{,}000$), purchased from Fluka, was used as received. Silver nitrate ($AgNO_3$), sodium borohydride ($NaBH_4$), and acetic acid were obtained from Shanghai Sanpu Chemical Co., Ltd. (China). Glutaraldehyde, supplied by Beijing Fuxing Chemical Reagent Factory (China), was diluted to a 30% (v/v) aqueous solution and used as crosslinking agents. All aqueous solutions were prepared with double distilled water. Pure AgNPs (average diameter <20 nm) was obtained from Wuhan Chemical Co., Ltd (China), for comparison study. All low-molecular weight materials are analytical-reagent grade and are used as received without further purification. Double distilled water was used throughout the experiment. *E. coli* (ATCC 44752), *B. subtilis* (ATCC 63501), *S. aureus* (ATCC 26003), and *P. aeruginosa* (ATCC 10110) were purchased from Beijing Center for Disease Prevention and Control.

Synthesis of AgNPs in Cts colloids

Acetic acid was diluted to a 0.02 g/mL aqueous solution and 4 g Cts was added to 100 mL of the above solution to form Cts solution. 1–5 mL of aqueous solution of $AgNO_3$ (0.1 mol/L) was mixed with 50 mL of the Cts solution, the obtained mixture solution was stirred at 30°C for 30 min until a pink solution formed. After that, freshly prepared aqueous solutions of $NaBH_4$ were added quickly into the above mixture solution, keeping stirring for another 90 min. To ensure the entire reduction, the amount of $NaBH_4$ was 1–5 times of metal salt. In the procedure, Ag-Cts colloids were obtained by chemical reduction of Ag^+ to the corresponding Ag^0 with $NaBH_4$ in the acetic acid solution of Cts. Then the Ag-Cts colloids were precipitated out with acetone, filtered, and washed, then dried in vacuum at 60°C for 48 h. After crosslinking in the glutaraldehyde gas at 37°C for 24 h, the yellow Ag-Cts composite were obtained.

Characterization experiments

Particle size and morphology were detected by a TEM (Tecnai G2 F20) and a SEM (Philips XL-30). Size distribution and number-average particle diameters were obtained via a laser particle size distribution instrument (3000HSA, Malvern Instr Co.). FTIR of the samples were recorded on spectrometer (Nicolet Impact NEXUS-670) in the range of 400–4000cm^{-1}. XRD patterns were recorded at 40 kV and 100 mA on Rigaku D/MAX-2500 diffractometer using Cu-K_a radiation ($\lambda = 0.15406$ nm). The patterns were taken over the diffraction angle range $2\theta = 10$–$90°$. A Varian Cary 100 Scan UV-visible system equipped with an integrating sphere (USRS-99-010) attachment was used to obtain UV-vis spectroscopy of AgNPs over a range of 300–500 nm. A UV-visible spectrophotometer (SP-723, Shanghai spectrum instruments Co., Ltd, China) was used to determine optical densities of the cultures at 460 nm (O.D.460) during aerobic incubation. XPS measurement was conducted with a PHI 5000C ESCA spectrometer (Perkin-Elmer) with an Al K_α radiation as the X-ray source, the C, N, O, F, and Ag contents on the surface of samples were determined by the instrument. TGA-DSC was performed in a NETZSCH STA 449C thermoanalyzer in air at a heating rate of 10°C/min from the room temperature to 220°C.

Assay for antimicrobial activities of resultant composite against microorganisms

Microbial tests were performed to examine the antimicrobial properties of the Ag-Cts composite against *E. coli*, *B. subtilis*, *S. aureus*, and *P. aeruginosa*. In the antimicrobial experiment the minimum inhibitory concentration (MIC) and the minimum bactericidal concentration (MBC) of the composite were determined. MIC is considered to be the lowest concentration of the composite that completely inhibits against bacteria comparing with the control, disregarding a single colony or a faint haze caused by the inoculum. MBC is taken to be the minimum concentration of the composite in the initial cultures that give cultures but the bacteria do not grow when re-inoculate into the nutrient broth.[23] The O.D. value method was used to determine the MIC and MBC of the Ag-Cts composite.[24] The minimum concentration of the composite that give cultures (or re-inoculated cultures) that did not become turbid was taken to be the MIC (or MBC).[23]

The suspensions of pure AgNPs, Cts powder, and Ag-Cts composite, were prepared in 0.01 g/mL

acetic acid. Duplicate serial dilutions of each sample were added to nutrient broth (beef extract 5 g, peptone 10 g, sodium chloride 5 g to 1000 mL distilled water, pH 7.2) for the final concentrations of 100–800 μg/mL. Control experiments were performed with 0.01 g/mL of acetic acid. Then they were autoclaved at 121°C for 25 min. The culture of *E. coli* was diluted by sterile distilled water to approximately 10^6 CFU/mL. A loop of each suspension was inoculated on nutrient medium with the sample or the control added. After inoculation, the plates were incubated at 37°C for 24 h. During the aerobic incubation, the optical densities at 460 nm (O.D.460) of the cultures were determined by a UV-visible spectrophotometer, and then the MIC and MBC values were obtained.

To study the bactericidal activity of the composite, each kind of microorganisms was grown overnight in 150 mL nutrient broth. All cells were harvested by centrifugation and suspended in 300 μg/mL nutrient broth. Three 100 μL portions of each cell suspension were inoculated into 50 mL volumes of nutrient broth, with original Cts or with Ag-Cts composite at a concentrations of 700 μg/mL. During aerobic incubation at 37°C for 24 h, the optical densities at 520 nm (O.D.520) of the cultures were determined using the UV-visible spectrophotometer. The numbers of colonies were counted according to the O.D. standard curves and the antimicrobial rates were obtained from the following equation:

$$\text{Antimicrobial rate} = (N_0 - N_1)/N_0 \times 100\% \quad (1)$$

where, N_0 and N_1 were referred to as the number of microorganism groups in the control culture plates and the experiment culture plates after aerobic incubation at 37°C for 24 h, respectively.

RESULTS AND DISCUSSION

Synthesis of AgNPs

Actually, the high performance of nanomaterials is achieved by controlling their phase structure in the nanosized range. The size and microstructure of nanoparticles are firmly dependent on the reaction conditions of synthesis system, such as the concentration of precursor ($AgNO_3$) and the ratio of oxidant and reducer ($AgNO_3$: $NaBH_4$). The UV-vis absorption spectra of Ag-Cts composites prepared with various concentrations of silver nitrate ($AgNO_3$: $NaBH_4$ = 1 : 3) are shown in Figure 1(a). It could be seen that the absorption peaks at approximately 410–430 nm corresponded well with that of pure AgNPs.[25] The color and the UV-vis absorption spectra density of the AgNPs colloid were dependent on the $AgNO_3$ concentration. As the concentration of $AgNO_3$ increasing, the color of the resultant colloid changed from bright yellow to light red and the absorption intensity increased accordingly, which meant the formation of more AgNPs. The final wavelength for the maximum absorption was also dependent on the initial silver ion concentration. They blue shifted from 415.8 nm to 409.4 nm when the $AgNO_3$ concentration increased from 0.27 g/L to 0.41 g/L, meaning that the particle size decreased. After that, the maximum absorption red shifted slightly when further increasing the $AgNO_3$ concentration to 0.51 g/L, suggesting that particle size increased due to the aggregation.[26]

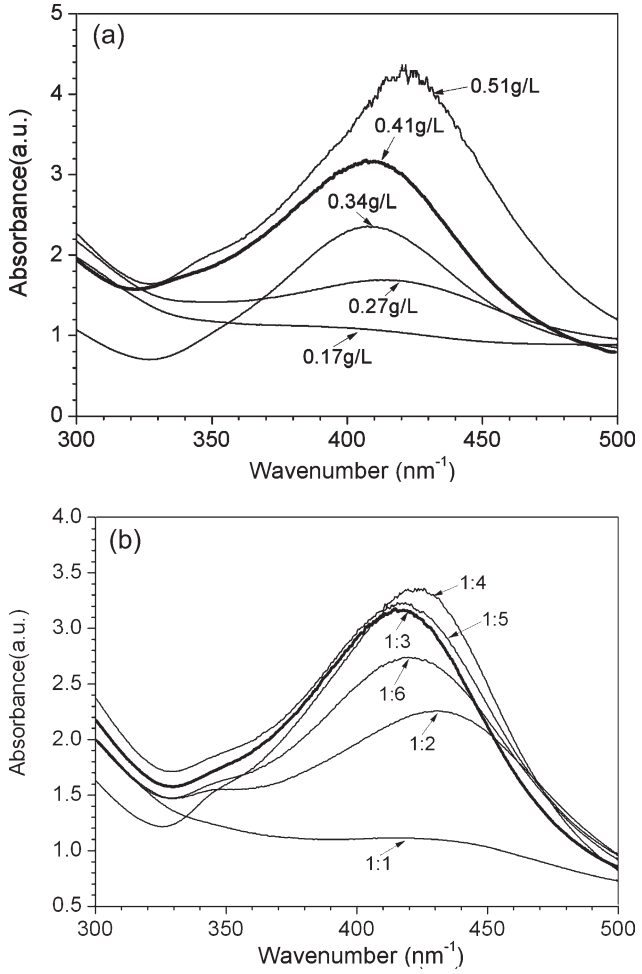

Figure 1 UV-vis absorption spectra of Ag-Cts composite prepared with various (a) concentrations of silver nitrate ($AgNO_3$: $NaBH_4$ = 1 : 3) and (b) molar ratio of $AgNO_3$ and $NaBH_4$ (C_{AgNO3} = 0.41 g/L).

These phenomena were believed to come from the reason that when $AgNO_3$ was mixed with Cts solution, Cts could chelated with Ag^+ by hydroxyl or amidogen groups and Ag^+ could be embedded in the Cts matrix, so AgNPs could disperse evenly in the colloids after Ag^+ reduced by $NaBH_4$ and AgNPs were in nanosize at the studied concentration range. The size of AgNPs was influenced by the

formation rate of Ag nuclei and the growth rate of Ag nanocrystals. At lower $AgNO_3$ concentration, the former was higher than the latter, so the size of AgNPs was decreased when $AgNO_3$ concentration added. When adding more $AgNO_3$ solution into reaction system, the case reversed.

The UV-vis spectra for Ag-Cts composites prepared at different molar ratios of $AgNO_3$: $NaBH_4$ (*N*) are shown in Figure 1(b). The absorption peaks at approximately 410–440 nm corresponded to that of AgNPs. When a small amount of $NaBH_4$ was used and *N* shifted from 1/1 to 1/3, the absorption intensity increased and the maximum absorption blue shifted, suggesting that the size of AgNPs was reduced. The reason was probably that the more amount of $NaBH_4$, the higher the reduction velocity and then the smaller size AgNPs formed. As *N* shifted from 1/4 to 1/6, the absorption intensity decreased and the maximum absorption position red shifted, suggesting the size of AgNPs increased due to the particle aggregation. It was because that when further increasing the amount of $NaBH_4$, the redundant BH_4^- ion could penetrate into Cts chains and break down the networks of Cts, which partly resulted in the aggregation of AgNPs.

Particle size and morphology

Transmission electron microscopy has provided the morphology and size details of AgNPs embedded in Cts matrix. A representative TEM image recorded from Ag-Cts composite is shown in Figure 2(a). In the image, the particles embedded in crosslinking Cts matrix are well separated and reasonably dispersed. An enlarged micrograph of the colloidal AgNPs in the inset box provided further insight into the morphology of the AgNPs in Cts colloids. The particles presented an elliptical spherical structure and their size was no more than 20 nm. The particle size distribution histogram of colloidal AgNPs in Figure 2(b), which obtained by measuring the size of about 1000 nanoparticles via a laser particle size distribution instrument, could be reasonably well fitted by a Gaussian curve. With the help of the histogram, the average particle size of AgNPs was counted to be 9 ± 5 nm and the result was consistent with that of XRD patterns (10.8 nm). As no other protective agents added in the synthesis system, Cts molecules acted as dispersant to prevent the growth and aggregation of particles in the synthesis process of AgNPs.

The resultant Ag-Cts particles were rather large and could be conveniently imaged using SEM. Figure 3 shows SEM picture of Ag-Cts particles prepared by crosslinking technology in the presence of AgNPs. The particles exhibited a regular spherical shape with the size of less than 10 μm. The surface

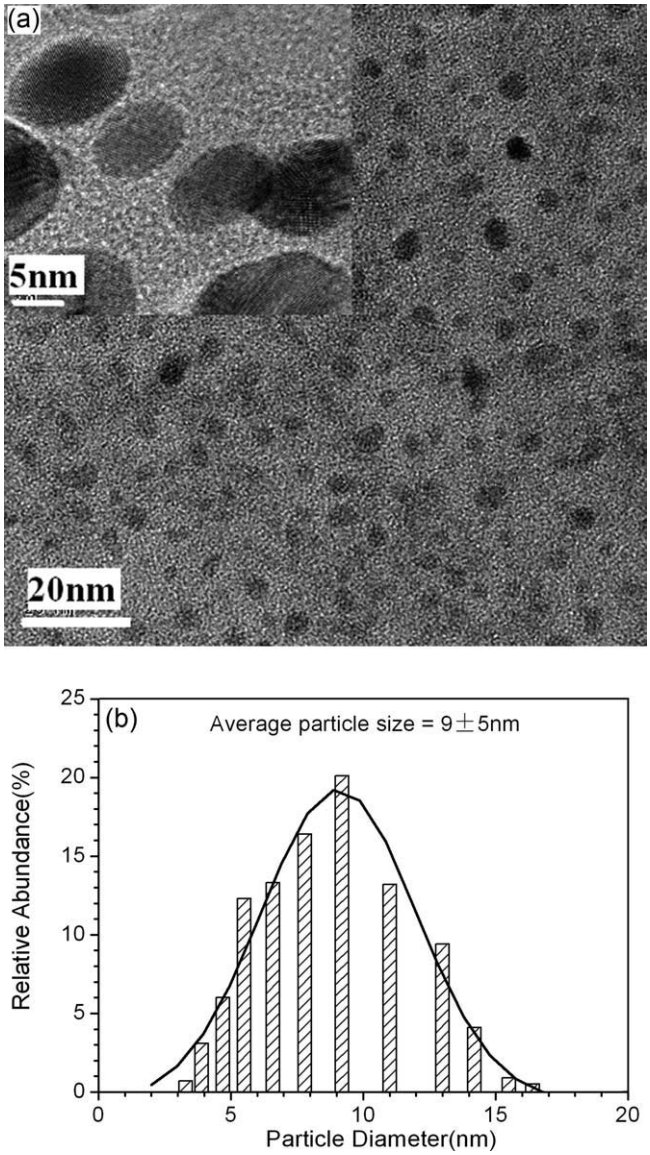

Figure 2 TEM images of colloidal Ag-Cts composite. An enlarged micrograph of the colloidal AgNPs was in the inset box (a) and histogram of particle size distribution shows the polydisperse nature of AgNPs (b).

of the particles was smooth and no Ag beads were detected on the whole surface of the samples. These observations could lead to the conclusion that the AgNPs were encapsulated into the Cts particles in the course of the crosslinking process.

FTIR analysis

To determine if chemical bond between the Cts matrix and the Ag nanoparticles exists, FTIR measurements of Ag-Cts composite, pure AgNPs, and original Cts were performed. The corresponding spectra are shown in Figure 4. The characteristic peaks of pure AgNPs at 1452 cm^{-1}[27] and original Cts at 1081 cm^{-1} representing C—O stretching bond could

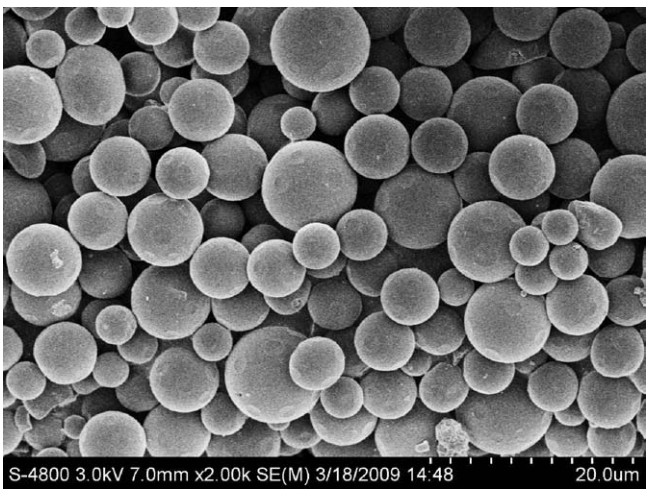

Figure 3 SEM image of Ag-Cts nanocomposite particles.

be found in the spectrum of the resultant composite.[28] The absorption peaks in the region 2800–3000 cm^{-1} corresponded to the —CH_2 and —CH_3 groups of Cts and the composite. It could be seen from Figure 4(c) that the peak of AgNPs at 1492 cm^{-1} [Fig. 4(a)] disappeared while the stretching peaks of —NH_2 group at 1598 cm^{-1} [Fig. 4(b)] shifted to 1567cm^{-1}. Such shifts in the IR values could be considered that —NH_2 or —OH groups of Cts combinated with Ag^+/Ag^0 by electrostatic bond similar to that described by Vigneshwaran et al.[29] Addtionally, the *N*—H scissoring band at 1659 cm^{-1} from the primary amine disappeared and the intensity of O-H stretching band at 3461 cm^{-1} from the hydroxyl decreased when silver loaded to the Cts chains, suggesting the chelation of Ag with both amino groups and hydroxyl of Cts, as shown in Figure 4(c). The above results confirm that the chemical bond exists between Cts molecules and Ag nanoparticles.

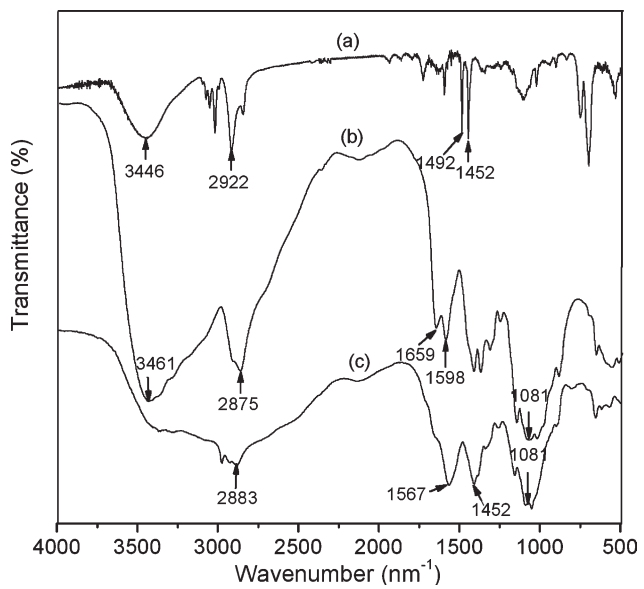

Figure 4 FTIR spectra of pure Ag, original Cts and Ag-Cts composites in wave number between 4000 cm^{-1} and 500 cm^{-1}. (a) pure AgNPs; (b) original Cts; (c) Ag-Cts composite.

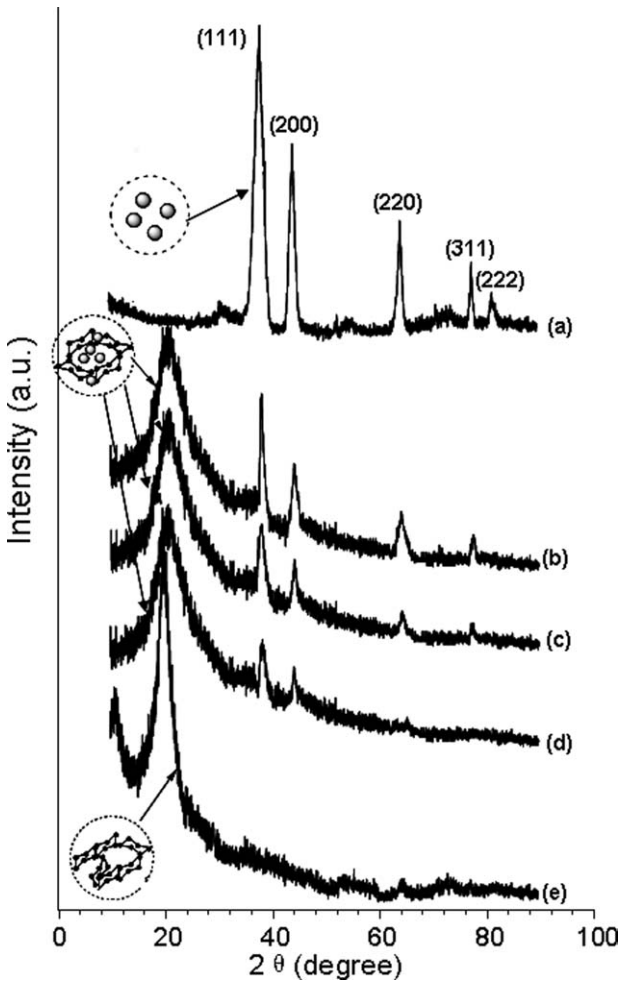

Figure 5 X-ray diffraction patterns of pure AgNPs, original chitosan and Ag-Cts composite. (a) pure AgNPs (purchased); (b), (c), and (d) are Ag-Cts composites with C_{AgNO3} = 0.51 g/L, 0.41 g/L, and 0.34 g/L in the synthesis systems, respectively; (e) original Cts.

X-ray diffraction analysis

Figure 5 shows XRD patterns of AgNPs, Ag-Cts composite, and original Cts. The broad reflexion at 22.57° is due to the crystallinity of original Cts.[28] The Bragg reflections at 38.16°, 44.28°, 64.38°, 77.74°, and 81.54° corresponded to the indexed planes of the crystals (111), (200), (220), (311), and (222) of Ag^0, Which pertain to a face centered cubic (fcc) lattice of silver.[30,31] In Figure 5(b–d), the three major characteristic peaks of Ag-Cts composite were corresponding with the crystal face of (111), (200), and (220) of AgNPs. The XRD of Ag-Cts composite showed similar pattern with that of pure Ag nanocrystal, which indicated the crystalline structure of

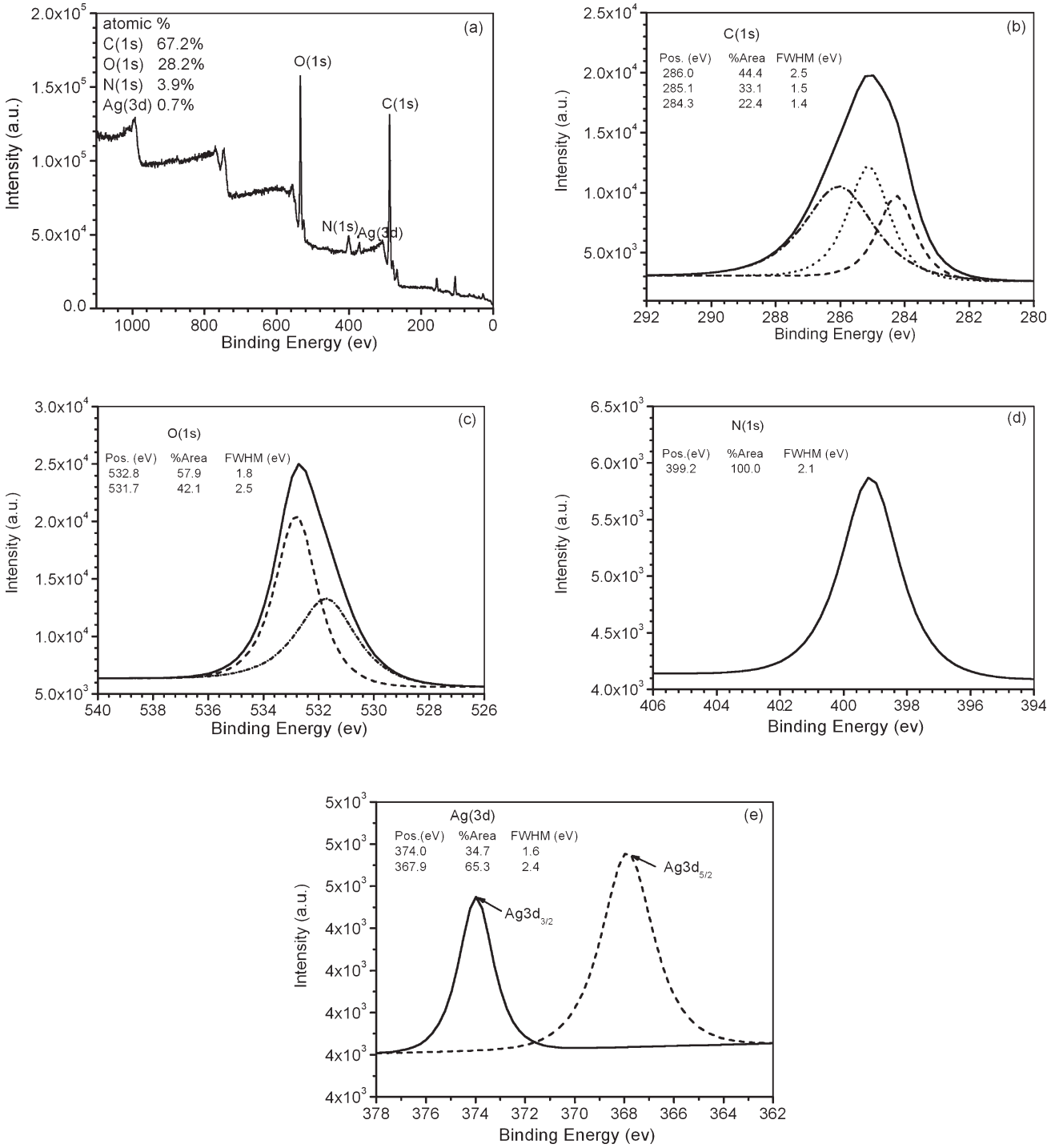

Figure 6 XPS spectra for Ag-Cts composite. (a) survey spectrum; (b) C1s; (c) O1s; (d) N1s; (e) Ag3d.

AgNPs did not change when they were introduced into Cts matrix. Since the content of AgNPs in Ag-Cts composite was very low the diffraction intensity of the silver was weak in the pattern of the composite.

According to the full width at half-maximum (FWHM) of the diffraction peaks, the average sizes of AgNPs in the composite with initial $AgNO_3$ concentrations of were estimated from the Scherrer equation (formula 2) to be about 10.8 nm (C_{AgNO3} = 0.27 g/L), 7.36 nm (C_{AgNO3} = 0.34 g/L), and 7.92nm (C_{AgNO3} = 0.41 g/L), respectively. The results were consistent with the TEM images.

$$D_{hkl} = k \times \lambda/(\beta_{hkl} \times \cos\theta_{hkl}) \quad (2)$$

where D_{hkl} is the particle size perpendicular to the normal line of (*hkl*) plane, k is a constant (it is 0.9),

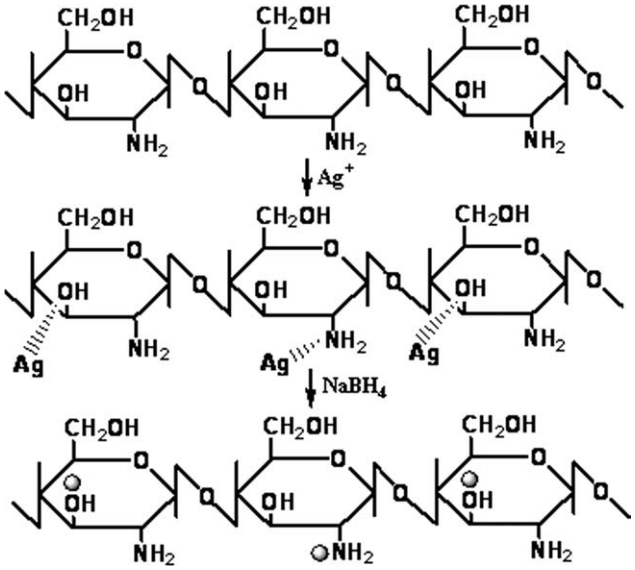

Figure 7 Schematic representation of *in situ* preparation of Ag-Cts composite (The filled circle denoted AgNPs).

β_{hkl} is the full width at half maximum of the (*hkl*) diffraction peak (it is 0.81), θ_{hkl} is the Bragg angle of (*hkl*) peak (it is 36.8°) and λ is the wavelength of X-ray (it is 0.15406nm).

XPS analysis

Figure 6(a) shows XPS spectrum of Ag-Cts composite after crosslinked by glutaraldehyde. The XPS analysis of the composite showed the presence of silver, nitrogen, oxygen, and carbon for the samples. The occurrence of an XPS peak at 399.2 eV for N1s [Fig. 6(d)] assigned to C—N bond derived from Cts in the composite. In Figure 6(e), the Ag3d peaks at 367.9 eV ($3d_{5/2}$) and 374.0 eV ($3d_{3/2}$) are characteristic of metallic Ag and Ag ion.[32] The presence of Ag^+ could result from the combining of AgNPs with the oxygen in the air or the solution. It also probably resulted from the interaction between AgNPs and the hydroxyl group in Cts molecules.

XPS spectra of C1s and O1s have been fitted by multiple Gaussians. Three peaks at 284.3eV, 285.1eV, and 286.0eV [Fig. 6(b)] for C1s can be assigned to the bonds of C—C, C—N, and C=O in the composite, respectively. In Figure 6(c), two peaks at 531.7eV, 532.8eV are for O1s.[33] The signals of O1s shifted to a higher binding energy, implying that the electron density decreased. Because no other impurities were detected within the sensitivity of the technique, the two peaks at 531.7eV, 532.8eV could be assigned to the bond of C—O and Ag—O in the composite, respectively. The Ag—O bond existing in the composite formed by the tight combination between a vacancy in the *d*-orbital of Ag and Cts molecules,[11] which are consistent with those of IR absorption values.

Based on the analysis results of XPS and FTIR, the preparation procedure of Ag-Cts composite could be summarized in Figure 7. In the structure of Cts the electron-rich oxygen and nitrogen atoms of polar hydroxyl and amidogen groups, respectively, are easily to interact with electropositive transition metal cations. Therefore, Ag^+ could interact with hydroxyl or amidogen groups of Cts macromolecules probably via electrostatic interactions at first. Then AgNPs were formed by the reduction of $AgNO_3$ with $NaBH_4$ in the presence of Cts and AgNPs were adsorbed by Cts molecules. After Cts crosslinked by glutaraldehyde, AgNPs dispersed evenly in the polymer matrix and the corresponding Ag-Cts composite were formed finally.

Thermal analysis of Ag-Cts composite

To study the thermal properties of the resultant composite, the TGA curves and DSC curves of Ag-Cts

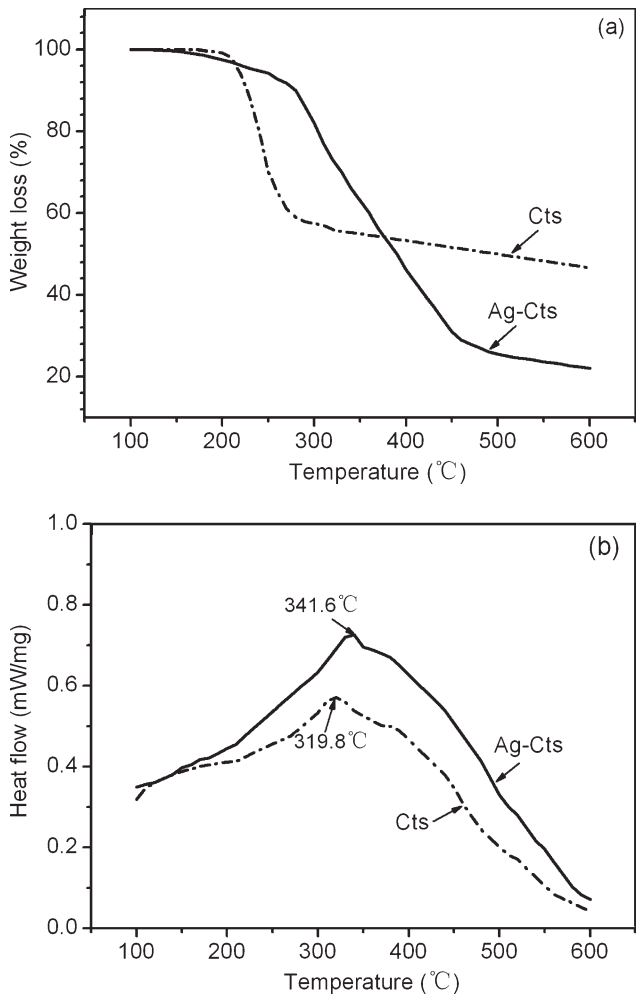

Figure 8 TGA curves (a) and DSC curves (b) of CS and Ag-Cts composite.

TABLE I
MIC and MBC of AgNPs, Original Cts and Ag-Cts Composite on Four Species of Bacteria

Bacteria	MIC (μg/mL)			MBC (μg/mL)		
	AgNPs	Cts	Ag-Cts	AgNPs	Cts	Ag-Cts
Escherichia coli (ATCC 44752)	250–300	800–1000	150–200	300–350	1200–1400	200–250
Bacillus subtilis (ATCC 63501)	200–250	800–1000	150–200	250–300	1200–1400	200–250
Staphylococcus aureus (ATCC 26003)	250–300	1000–1200	200–250	350–400	1400–1600	300–350
Pseudomonas aeruginosa (ATCC 10110)	400–500	1000–1200	300–400	600–700	1200–1400	500–600

composite and original Cts are shown in Figure 8. As seen in TGA curves [Fig. 8(a)], the decomposed rate of Cts was significantly higher than that of Ag-Cts at about 300°C and the mass loss of Ag-Cts was very low. It also can be found from DSC curves in Figure 8(b) that the decomposed temperature of original Cts was 319.8°C while the Ag-Cts composite did not decompose before 341.6°C. These results demonstrated that the thermal stability of Cts enhanced when loaded with AgNPs, which are in agreement with the thermal behaviors of Ag-polymer nanocomposites reported by Singh and Khanna[11] and Zhang et al.,[34] respectively.

The higher thermal stability of Ag-Cts composite could be attributed to the higher surface energy of AgNPs. Because of the higher surface energy, AgNPs combined with the oxygen in the air or water and then the united oxygen could integrate with hydrogen to form hydrogen bond, which could reduce the mobility of Cts chains in the composite. The chain mobility reduction could suppress the chain transfer reaction and slow the degradation process of Cts, and so the decomposition of Cts could take place at higher temperatures. Similar consequences about the synthesis of PVA-Ag nanocomposites have been explained by Mbhele et al.[35] Since there was only approximately 1 wt % content of AgNPs in the composite, the elevation of the decomposed temperature was limited.

Antimicrobial activities of resultant composite against microorganisms

The effects of the Ag-Cts composite (obtained with 0.41 g/L silver nitrate and the molar ratio of $AgNO_3$ and $NaBH_4$ was 1 : 3 in the synthesis system) on the growth of *E. coli, B. subtilis*, *S. aureus*, and *P. aeruginosa* were investigated by monitoring culture turbidity. Inhibition with 0.01 g/mL acetic acid was negligible and using it for the dispersion of the nanocomposite did not have any additional adverse effect on bacterial growth, so control experiments were performed with acetic acid aqueous solution. MICs and MBCs of the samples on four species of bacteria are shown in Table I. Growth of bacteria was controlled over the MICs of Ag-Cts. The MICs and MBCs of the Cts alone for the bacteria were higher than that of pure AgNPs, but the corresponding data of Ag-Cts composite were lower than that of pure AgNPs. For example, the MIC and MBC of Ag-Cts nanocomposite for *E. coli* were 150–200 μg/mL and 200–250 μg/mL, while those of pure AgNPs were 200–400 μg/mL and 400–600 μg/mL, respectively. Considering AgNPs were parts of the composite, the actual MIC and MBC of AgNPs in the antimicrobial suspension were only 1.54–2.05 μg/mL and 2.05–2.56 μg/mL, respectively. Thus the MIC and MBC for AgNPs are less than the corresponding values in other reports.[36]

Figure 9 shows the antimicrobial effects of pure AgNPs, Cts alone and Ag-Cts composite at a concentration of 700 μg/mL on four species of bacteria. Results showed that the antimicrobial rates of original Cts were greatly improved by the introduction of AgNPs and Ag-Cts composite had a wide spectrum of antimicrobial activities. Therefore, the complex of AgNPs and Cts can improve antimicrobial activities greatly in comparison with the single one of them.

Much hypothesis for antimicrobial mechanism of Ag on microorganisms has been reported. Recently, Kim, et al. proposed the mechanism for the inhibitory effects of Ag on microorganisms by electron

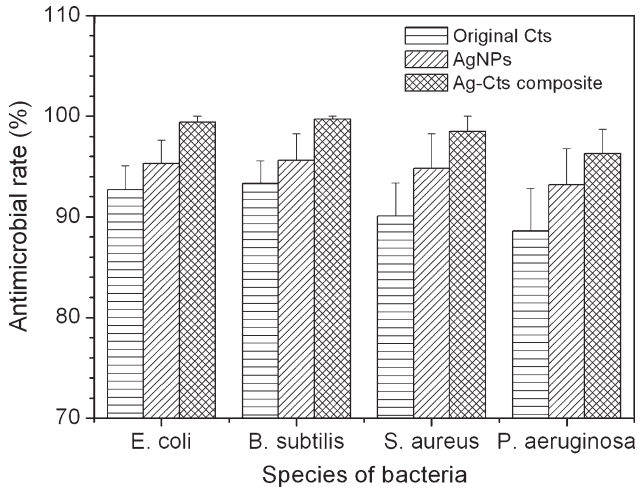

Figure 9 Relationship of antimicrobial rates for pure AgNPs, original Cts and Ag-Cts nanocomposites to four species of microorganisms.

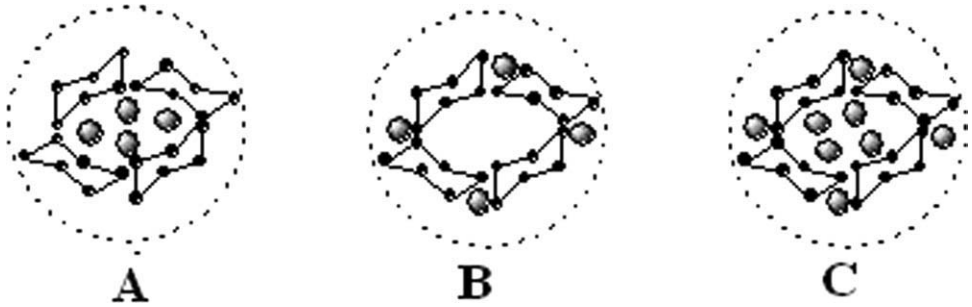

Figure 10 Possible structures of Ag-Cts nancomposite particles.

spin resonance spectroscopy and antioxidant study of AgNPs. They confirmed that free radicals could be derived from the surface of AgNPs and uncontrolled generation of free radicals could attack membrane lipids of microorganisms, then led to a breakdown of membrane function.[37] The AgNPs embedded in the resultant composite were about or less than 10 nm in diameter and the particles with smaller sizes were known to be reactive and hence could be efficient in their antimicrobial activities.[9] In fact, some AgNPs were encapsuled incompletely by Cts. The possible structures of Ag-Cts nanocomposite particles are shown in Figure 10. Because of the above mechanism, AgNPs in structure C and B are better than that in structure A for bacterial inactivation or germicidal action. Moreover, in the antimicrobial experiment of Ag-Cts nanocomposite Cts could adhere onto the microorganism cell wall to destabilize it and alter cell permeability, at the same time the networks of Cts let down and AgNPs encapsuled by Cts (structure A and C) come out to be responsible for subsequent free radical-induced membrane damage.

Cts itself is known to have strong antibacterial properties.[38] The proposed mechanism for the inhibitory effects of Cts on microorganisms is that the bacteria cell surfaces are negatively charged and when the bacteria cell wall is adsorbed on the cationic antimicrobial (Cts), it can bind and disrupt the cytoplasmic membrane of bacteria. With consequent destabilization of the cell envelope and altered permeability, the release of cytoplasmic constituents, such as DNA and RNA, to take place continuously, eventually the replication of DNA inhibited and all these leading to the death of the bacteria.[39,40] As Ag-Cts nanocomposite particles can attach to the bacteria cell wall by electrostatic interaction of Cts and the negatively charged bacteria cell, the cationic biocidal of it is expected to be antimicrobial. The present investigation therefore indicated that the composite was more efficient than either AgNPs or Cts alone for inactivating bacteria, owing to synergistic effect of both the AgNPs and Cts in the composite.

CONCLUSIONS

Results showed that AgNPs with well-controlled shape and size had little aggregation with the protection of Cts colloids and they dispersed well in cross-linking Cts matrix. SEM picture detected that Ag-Cts particles exhibited a regular spherical shape with the size less than 10 μm and AgNPs were encapsulated in the Cts particles. Moreover, thermal analysis of the resultant composite demonstrated that the thermal stability of Cts could be improved by the present of AgNPs since it could reduce the mobility of Cts chains in the composite. Microbial experiment indicated that the Ag-Cts composite exhibited excellent antimicrobial properties with Ag nanoparticles participating in the activities. The resultant Ag-Cts composite could be suitable for biological applications in medical treatment and sanitation fields.

References

1. Yu, D. G. Colloids Surf B 2007, 59, 171.
2. Dubas, S. T.; Kumlangdudsan, P.; Potiyaraj, P. Colloids Surf A 2006, 289, 105.
3. Kang, H. Y.; Jung, M. J.; Jeong, Y. K. Korean J Biotechnol Bioeng 2000, 15, 521.
4. Kalele, S. A.; Ashtaputre, S. S.; Hebalkar, N. Y.; Gosavi, S. W.; Deobagkar, D. N.; Deobagkar, D. D.; Kulkarni, S. K. Chem Phys Lett 2005, 404, 136.
5. Yoshida, K.; Tanagawa, M.; Atsuta, M. Biomed J Mater Res 1999, 47, 516.
6. Alt, V.; Bechert, T.; Steinrücke, P.; Wagener, M.; Seidel, P.; Dingeldein, E.; Domann, E.; Schnettler, R. Biomaterials 2004, 25, 4383.
7. Breuzard, G.; Angiboust, J. F.; Jeannesson, P.; Manfait, M.; Millot, J. M. Biochem Biophys Res Commun 2004, 320, 615.
8. Suber, L.; Sondi, I.; Matijevic, E.; Goia, D. V. J Colloid Interface Sci 2005, 288, 489.
9. Gogoi, S. K.; Gopinath, P.; Paul, A.; Ramesh, A.; Ghosh, S. S.; Chattopadhyay, A. Langmuir 2006, 22, 9322.
10. Julio, B. G.; Armando, J. S.; Hugo, F. L. J Appl Polym Sci 2008, 107, 45.
11. Singh, N.; Khanna, P. K. Mater Chem Phys 2007, 104, 367.
12. Jung, B. O.; Lee, Y. M.; Kim, J. J.; Choi, Y. J.; Jung, K. J.; Chung, S. J. J Korean Ind Eng Chem 1999, 10, 660.
13. Saint, S.; Elmore, J. G.; Sullivan, S. D.; Emerson, S. S.; Koepsell, T. D. Am J Med 1998, 105, 237.
14. Khor, E.; Lim, L. Y. Biomaterials 2003, 24, 2339.

15. Rhoades, J.; Roller, S. Appl Environ Microbiol 2000, 66, 80.
16. Yoshizuka, K.; Fujikawa, K.; Inoue, K. J Membr Sci 1997, 137, 201.
17. Vigneshwaran, N.; Nachane, R. P.; Balasubramanya, R. H.; Varadarajan, P. V. Carbohydr Res 2006, 341, 2012.
18. Chen, S. P.; Wu, G. Z.; Zeng, H. Y. Carbohydr Polym 2005, 60, 33.
19. Huang, H. Z.; Yang, X. R. Biomacromolecules 2004, 5, 2340.
20. Zhan, X. J.; Xiong, Y. Z.; Liu, Z.; Xie, D. Z. China J Biochem Pharmacol 2002, 22, 142.
21. Huang, H. Z.; Yang, X. R. Carbohydr Res 2004, 339, 2627.
22. Twu, Y. K.; Chen, Y. W.; Shih, C. M. Powder Technol 2008, 185, 251.
23. Speciale, A.; Musumeci, R.; Blandino, G.; Milazzo, I.; Caccamo, F.; Nicoletti, G. Int J Antimicrob Agents 2002, 19, 111.
24. Park, J. S.; Kim, J. H.; Nho, Y. C.; Kwon, O. H. J Appl Polym Sci 1998, 69, 2213.
25. Li, T.; Park, H. G.; Choi, S. H. Mater Chem Phys 2007, 105, 325.
26. Courrol, L. C.; Oliveira-Silva F. R., Gomes, L. Colloids Surf A 2007, 305, 54.
27. Zhao, Y.; Jiang, Y. J.; Fang, Y. Spectrochim Acta A 2006, 65, 1003.
28. Fan, L. H.; Du, Y. M.; Zhang, B. Z.; Yang, J. H.; Zhou, J. P.; Kennedy, J. F. Carbohydr Polym 2006, 65, 447.
29. Vigneshwaran, N.; Ashtaputre, N. M.; Varadarajan, P. V.; Nachane, R. P.; Paralikar, K. M.; Balasubramanya, R. H. Mater Lett 2007, 61, 1413.
30. Bogle, K. A.; Dhole, S. D.; Bhoraskar, V. N. Nanotechnology 2006, 17, 3204.
31. Prasad, V.; D'Souza, C.; Yadav, D.; Shaikh, A. J.; Vigneshwaran, N. Spectrochim Acta A 2006, 65, 173.
32. Huang, H. H.; Ni, X. P.; Loy, G. L.; Chew, C. H.; Tan, K. L.; Loh, F. C.; Deng, J. F.; Xu, G. Q. Langmuir 1996, 12, 909.
33. Xu, J.; Han, X.; Liu, H. L.; Hu, Y. Colloids Surf A 2006, 273, 179.
34. Zhang, K.; Fu, Q.; Fan, J. H.; Zhou, D. H. Mater Lett 2005, 59, 3682.
35. Mbhele, Z. H.; Salemane, M. G.; Sittert, C. G. C. E.; Nedeljkovic, J. M.; Djoković, V.; Luyt, A. S. Chem Mater 2003, 15, 5019.
36. Sanpui, P.; Murugadoss, A.; Durga-Prasad, P. V.; Ghosh, S. S.; Chattopadhyay, A. Int J Food Microbiol 2008, 31, 142.
37. Kim, J. S.; Kuk, E.; Yu, K. N.; Kim, J. H.; Park, S. J.; Lee, H. J.; Kim, S. H.; Park, Y. K.; Park, Y. H.; Hwang, C. Y.; Kim, Y. K.; Lee, Y. S.; Jeong, D. H.; Cho, M. H. Nanomed Nanotechnol Biol Med 2007, 3, 95.
38. Sarasam, A. R.; Brown, P.; Khajotia, S. S.; Dmytryk, J. J.; Mad, S. V. J. Mater Sci Mater Med 2008, 19, 1083.
39. Cuero, R. G.; Osuji, G.; Washington, A. Biotechnol Lett 1991, 13, 441.
40. Feng, Q. L.; Wu, J.; Chen, G. Q.; Cui, F. Z.; Kim, T. N.; Kim, J. O. J Biomed Mater Res 2000, 52, 662.